N82 26072

349

HARD X-RAY IMAGING FROM EXPLORER

J. E. Grindlay and S. S. Murray
Harvard-Smithsonian Center for Astrophysics

ABSTRACT

Hard X-ray Astronomy (at energies $\gtrsim$10 keV) has not yet enjoyed the high sensitivity and high resolution that imaging techniques and the Einstein Observatory have allowed for the soft X-ray band. Many fundamental problems in high energy astrophysics require greatly increased sensitivity and observing time at hard X-ray energies. It is possible to obtain such large increases in sensitivity as well as angular resolution with coded aperture imaging X-ray detectors. A new hard X-ray coded aperture detector concept is described which would enable very high sensitivity studies of persistent hard X-ray (~15-300 KeV) sources and gamma ray bursts (~50-550 KeV). Coded aperture imaging is employed so that ~2′ source locations can be derived within a 3° field of view. Gamma bursts could be located initially to within ~2° and X-ray/hard X-ray spectra and timing, as well as precise locations (~2′), derived for possible burst afterglow emission. Hard X-ray imaging should be conducted from an Explorer mission where long exposure times are possible.

1. INTRODUCTION

With the Einstein Observatory, soft X-ray astronomy has become fully competitive with optical and radio astronomy in that virtually all major classes of astronomical object have proven to be detectable in this energy band. Such spectacular growth has not yet occurred in hard X-ray astronomy. However, the results which are available suggest a rich variety of astrophysical problems. For example, although Einstein observations have revealed that quasars and active galactic nuclei (AGN) are almost always detectable in (soft) X-rays, their spectra and hence source radiation mechanisms are still largely unknown. In the few brightest quasars, and in a somewhat larger number of still brighter Seyfert galaxies, hard X-ray emission extending out to at least several hundred keV is detected. Most of the radiation and luminosity from quasars and AGNs may be in the hard X-ray band, and thus realistic models will not be possible until many high quality X-ray observations at energies up through the probable high energy spectral break (at ~200-300 keV) are available.

In addition to the quasars, a number of other fundamental problems in high energy astrophysics may also be studied, and in some cases understood, best in the hard X-ray band. The scientific need for high sensitivity and high angular resolution at hard X-ray energies (~10-500 keV), as discussed in the next section, could be met with a coded-aperture imaging detector. An Explorer-class hard X-ray imaging experiment would be the ideal compliment to future direct imaging X-ray telescopes (e.g., EXOSAT, ROSAT, AXAF, and eventually, LAMAR) which will, of course, be sensitive only below ~5-8 keV.

2. SCIENTIFIC NEED FOR HARD X-RAY OBSERVATIONS

A wide range of fundamental problems in astrophysics can best be attacked with sensitive new observations at hard X-ray energies. It is possible to summarize these in the form of a table of particular problems and the approximate ranges of photon energies required for their solution. Table 1 contains such a summary, in which each entry is an area of study which requires observations in the photon energy range shown. Arrow tips mean that the energy limit (high or low) is not well determined, whereas vertical ticks at the energy range ends mean that the range is more or less fixed.

In the general study of compact objects hard X-ray spectra can provide a key test for the nature of the object. White dwarfs would not be expected to have thermal spectra with temperatures above the free full temperatures of ~200 keV whereas neutron stars could have thermal components extending to MeV energies. X-ray bursts have shown that neutron star radii can be measured from the blackbody spectra at low energies whereas recent gamma ray burst studies by the Soviets at ~30-500 keV suggest that the 511 keV annihilation line has been detected at a gravitational redshift of ~0.2-0.3, or approximately that expected for a neutron star. Cyclotron lines have been detected at hard X-ray energies (~60 keV) and neutron star magnetospheres might be studied at either hard (~100-200) energies corresponding to local free full temperatures at the Alfven radius or soft (~0.3 keV) energies if there is optically thick re-emission.

Accretion flows and the distribution of cool gas and hot electrons in accreting systems require hard X-ray observations. In particular, the study of Comptonization of a soft spectral component by energetic electrons can lead to hard Compton-tails out to several hundred keV. The resulting power law - type spectra and thermal cutoffs might be expected in many more objects than just Cyg X-1 where they have been observed. Studies of the simultaneous variations in the soft vs. hard X-ray spectra as a function of binary phase might allow the spatial temperature and density structure of the accretion flow to be studied.

Determination of the radiation mechanisms involved in given X-ray sources obviously requires broad band spectra extending to hard energies. Thermal cutoffs at high energies can distinguish Comptonization of thermal spectra from non-thermal processes. Sources with predominantly ~10 keV thermal bremsstrahlung spectra (e.g., most galactic bulge sources) may be expected to have underlying hard components from thermal processes (free fall, Comptonization, etc.) or non-thermal particle acceleration as in SS433.

Finally, and perhaps most important, the basic understanding of any object requires knowing its luminosity and overall energetics. For quasars and active galactic nuclei (AGN) in general, this requires hard X-ray observations since the spectra already observed from the few brightest sources indicate that the hard band (>100 keV) contains a large fraction of the total energy radiated. It is not possible to

Table 1

QUESTIONS IN X-RAY ASTRONOMY vs. ENERGY

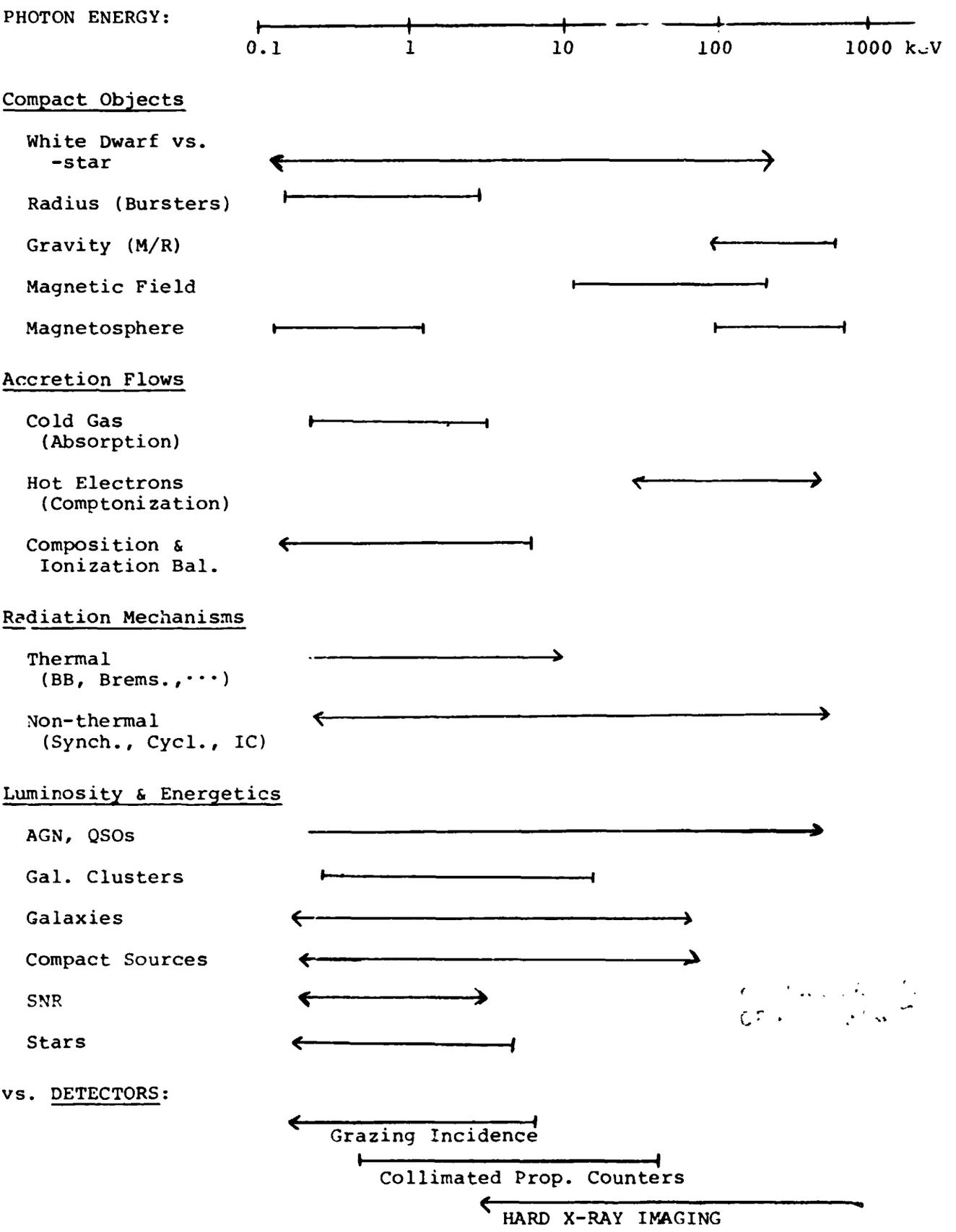

construct meaningful models for quasars without knowing where (and why) their spectra finally cutoff at high energies. Galaxy clusters must emit some level of inverse Compton radiation from synchrotron radio electrons scattering on the microwave background. This should extend to hard energies and its detection would constrain the energetics of relativistic gas in galaxy clusters. At somewhat lower luminosities, emission from normal galaxies and compact objects have hard X-ray components which are almost certainly significant whereas SNR and stars probably have negligible luminosity at hard X-ray energies.

At the bottom of Table 1, we give the approximate energy ranges of the principal detector systems used to attack the problems discussed above. It is clear that grazing incidence imaging, as used on Einstein, cannot deal with a significant number of these major problem areas, nor can collimated proportional counters of the sort employed in all X-ray astronomy missions thus far. Hard X-ray imaging, however, could attack all of the major problems.

3. CODED APERTURE SYSTEMS FOR HARD X-RAY IMAGING

At energies above the grazing incidence limit of ~10 keV, X-ray imaging can be accomplished by at least two techniques. Bragg diffraction flux concentrators can be employed to achieve large effective detector areas with small detecting elements (and thus detector backgrounds). Such a system is described by Ricker (1981) but it is limited to energies $\lesssim$100 keV. For the broad-band studies described above, where good sensitivity and angular resolution up to ~500 keV is desired, it appears that coded aperture imaging is the optimum technique. This scheme employs an aperture, with an array of transmitting holes, followed by a position-sensitive detector. It is thus just the multiple pinhole camera proposed by Dicke (1968). Images are reconstructed (uniquely) by, essentially, re-projecting each detected photon back through each open mask hole. All counts from a given source are detected in the true image pixel although (in contrast to true imaging) the total background (including sources) is also necessarily re-projected into each image pixel. For imaging hard X-rays, the requirement that the detector and mask planes be parallel and the detector be thin (for minimum detected position ambiguity and thus image smearing) means that crystal scintillators are preferred for the detector. Position-sensitive detection of the optical light produced by a hard x-ray in a crystal scintillator is then the technical requirement for a coded aperture hard X-ray imaging detector. We shall describe in the next sections a proposed detector in some detail.

First, we summarize the main advantages of a coded aperture system for hard X-rays. The angular resolution can be high, and is just the angular spacing of mask holes (which become image elements) as seen from the detector. Thus source confusion in crowded fields (e.g., the galactic center region) can be eliminated. The field of view can be large although the diffuse background is then also large,

but must be commensurate with the number of image elements and their angular size as governed by the mask. Finally, and most important, the detected background can be measured simultaneously with a source by simply comparing the rates in the reconstructed image in and out of the pixel(s) of interest containing the source(s). This means, of course, that continuous pointings of long exposure can be carried out for very large increases in sensitivity over previous scanning detectors such as HEAO-A4. This is also an improvement over detectors which chop on and off source (e.g., the NRL experiment on GRO) since chop times must always be shorter than the (uncertain) timescales for background variations if these are to be removed.

In Figure 1 we compare the approximate sensitivity that a plausible coded aperture hard X-ray imaging detector system might give relative to the sensitivities achieved with HEAO-1 and HEAO-2. The hard X-ray imaging experiments will, in general, not be designed to operate below ~10 keV (the domain of normal imaging X-ray telescopes) and will not perform as well above ~500 keV-1 MeV, where Compton scattering and pair production in the mask become significant. Sensitivities could be achieved (from an Explorer mission) in the ~10-500 keV range which are at least a factor of 10-30 greater than available previously above 10 keV even for the modest-sized hard X-ray imaging experiment described next.

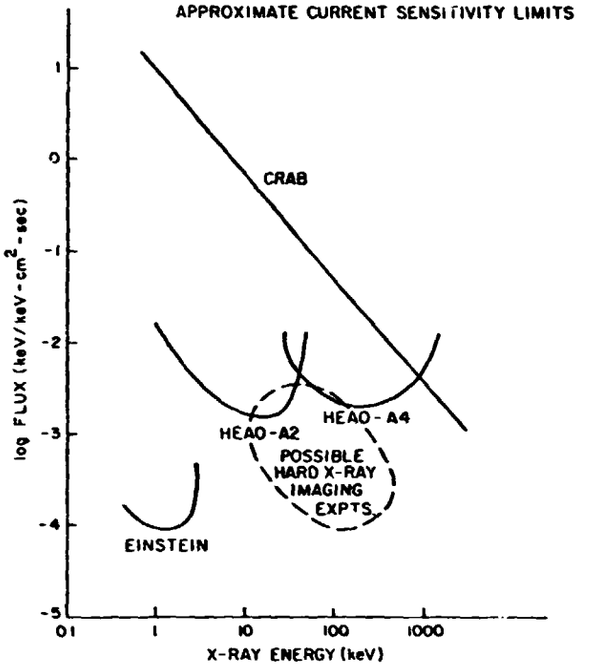

Figure 1: Approximate relative sensitivity of X-ray experiments and the Crab spectrum for comparison.

4. PROPOSED HARD X-RAY IMAGING EXPERIMENT

We now describe a particular experiment configuration for hard X-ray imaging from an Explorer. This is the Energetic X-ray Imaging and Timing Experiment (EXITE) which was proposed as a second experiment to XTE. Either this experiment as proposed, or an enlarged version (EXITE is modular) for an entire Explorer mission, would enable the major astrophysical problems discussed above (cf. Table 1) to be studied in detail.

The scientific objectives (in abbreviated form) of EXITE are: (1) to measure Comptonization tails and cyclotron features in source

spectra to determine physical conditions at the source; (2) to measure spectral-temporal variability at high energies and study accretion flows; (3) to locate and identify hard X-ray sources in complex fields; (4) to measure high energy spectra of quasars and locate serendipitous sources; and (5) to measure the size spectrum (log N - log S), broad energy spectrum (including line emission) and source locations for gamma ray bursts.

General Description of EXITE

EXITE represents a fundamentally new concept in hard X-ray astronomy. It applies coded aperture imaging to the hard X-ray band (~15-300 KeV) and at once realizes several key advantages mentioned above which were previously only possible at low X-ray energies: (1) background is measured simultaneously with the object flux; there is no need to scan or off-set point; (2) a source can be resolved in complex fields; and (3) precise (~2-5 arcmin) positions can be derived for the first time at hard X-ray energies (~100 KeV) by centroiding between resolution elements of the reconstructed image.

Coded aperture imaging systems are based on the multiple pinhole camera (Dicke 1968) where N overlapping images of a source distribution are formed on a detector viewing the source through N pinholes in an aperture mask. Although Dicke suggested using a random hole pattern, images reconstructed using a "random" pattern (never truly random) contain an additional source of systematic noise. To overcome this we suggested (in a 1976 Spacelab 2 proposal) using a "pseudo-noise" (PN) array since these have the optimum property (Calabro and Wolf 1968) that their autocorrelation function (ACF) is identically constant off axis and a δ-function on axis. PN arrays were independently pointed out by Gunsen and Polychronopulos (1976) and have been discussed extensively by Fenimore (1980, and references therein) who call them uniformly redundant arrays (URA). The (systematic) noise-free imaging possible with a URA mask is not compromised by a physical realization of such a pattern where the hole size is smaller than the hole spacing. Furthermore, the URA is cyclic and has the very desirable "window property" that a complete pattern is available to surround every element of an extended mask.

The EXITE detector makes optimum use of these desirable properties of the URA in that each single detector (a 15 cm diameter CsI scintillator crystal) views the sky through a URA mask composed of a number (~50) of contiguous cycles of a basic URA pattern (each of dimension 13 x 11; see Figure 2). A single detector, which is read out as one device, then effectively (in the analysis) produces ~50 independent and parallel 13 x 11 pixel images which are then co-added. This allows a very much

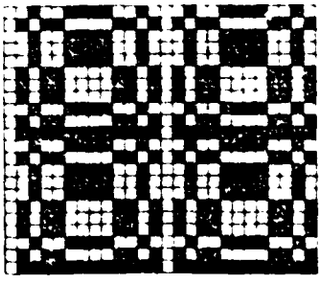

Figure 2: A 2 x 2 Cycle Portion of the Extended URA Coded Aperture Collimator.

faster analysis (by a factor of 50) of the total image than if the entire detector area viewed the entire URA mask as in a "conventional" coded aperture camera. The mosaicing of the detector and mask also allows the optimum packing of the rectangular URA pattern into the round detector elements required (because of the need for a diode image intensifier tube to amplify the scintillator optical output). Finally, the URA mask is made self-supporting by placing the (1.5 mm square) holes on a 1.7 mm grid. This is turned to additional advantage by using the 1.5 mm holes as the detector collimator. Collimation (2.9° FWHM) is achieved by making the mask effectively very thick (3 cm) using spaced tungsten laminates (see Figure 3).

Design Principles and Operation of EXITE

The principles of operation of the EXITE detector are illustrated in Figure 4. The URA mask projects a collimated image of the sky onto a CsI scintillator. The light produced in the CsI scintillator by an incident X-ray is amplified by the intensifier while preserving the spatial distribution of brightness. The intensified image is decreased in scale to match the input of the MAMA detector through a reducing fiber-optic (12:1). The light losses in this reduction are compensated by the gain of the intensifier so that the total number of photons incident on the photon-counting imaging detector is the same as initially collected from the scintillator. This preserves the energy resolution capability of the system which is basically limited by the counting statistics of the light from the CsI. The imaging optical detector required could be a resistive anode (Martin et al. 1981) crossed grid (Kellogg, Murray, and Bardas 1979) or multi-anode (Timothy, Mount, and Bybee 1979) type system. The Multi-Anode-Microchannel-Array (MAMA) detector (Timothy, Mount, and Bybee 1979) is especially well suited for EXITE and, therefore, included in the design here.

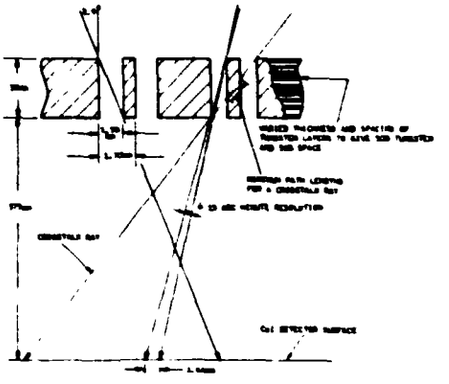

Figure 3: Laminated Tungsten Coded Aperture Collimator.

The anodes of the MAMA detector are 140 μm x 140 μm which corresponds to the hole spacing in the URA mask (1.7 mm) when the reduction factor of 12:1 is considered. Light reaching the MAMA from a single X-ray results in the production of a few tens to several hundreds of photoelectrons depending on incident energy. These will be spread out over several of the 140 μm pixels due to the thickness of the CsI crystal and the front window of the image intensifier. Thus, several of the anode lines along each axis will detect the event. A centroid estimate of the event position is then determined for each axis by the processing electronics. Since the photoelectrons are spread out on a large scale relative to the MCP channel size

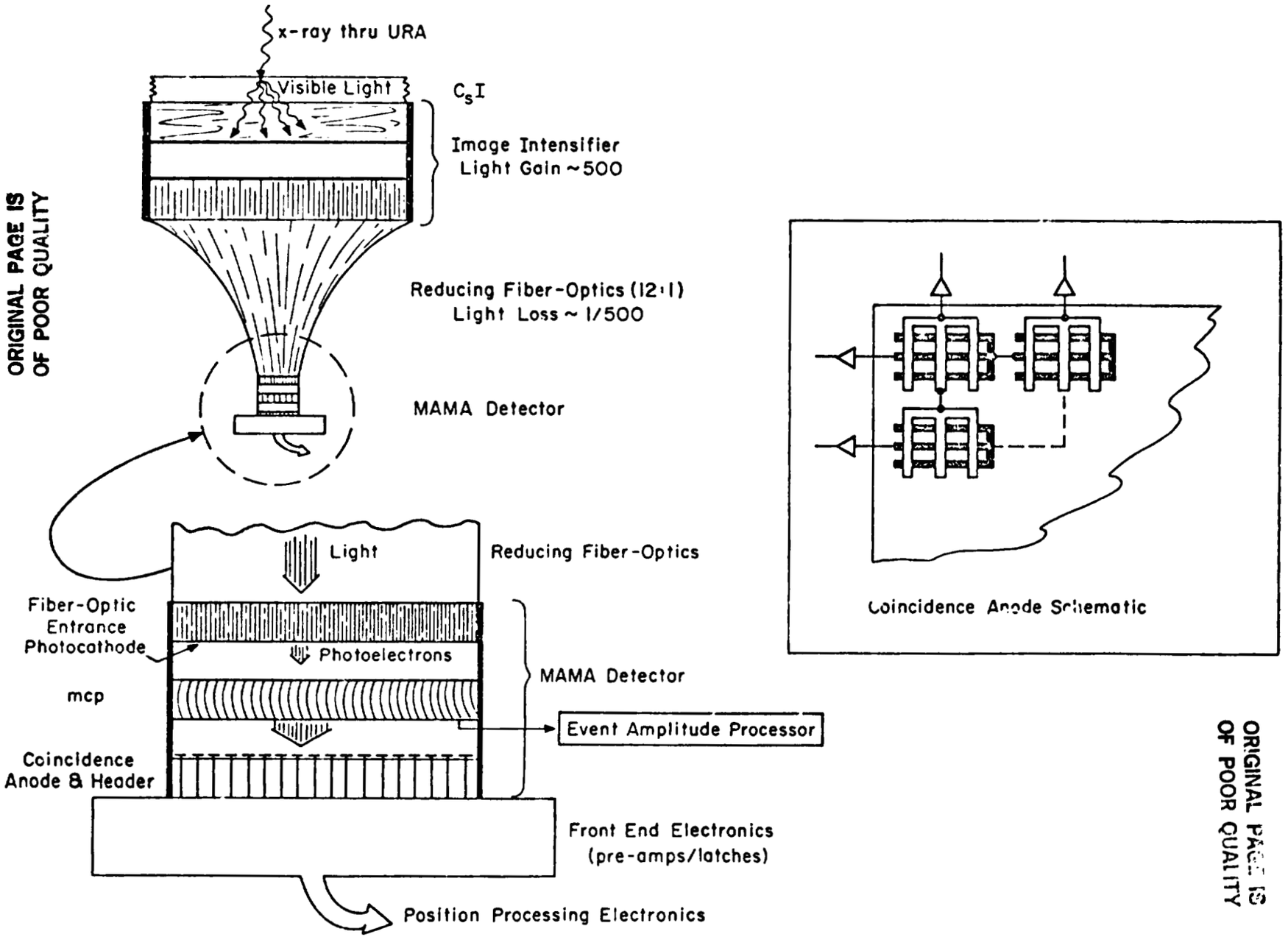

Figure 4: Schematic of Position-Sensitive Scintillation Detection with Optical Imaging Readout.

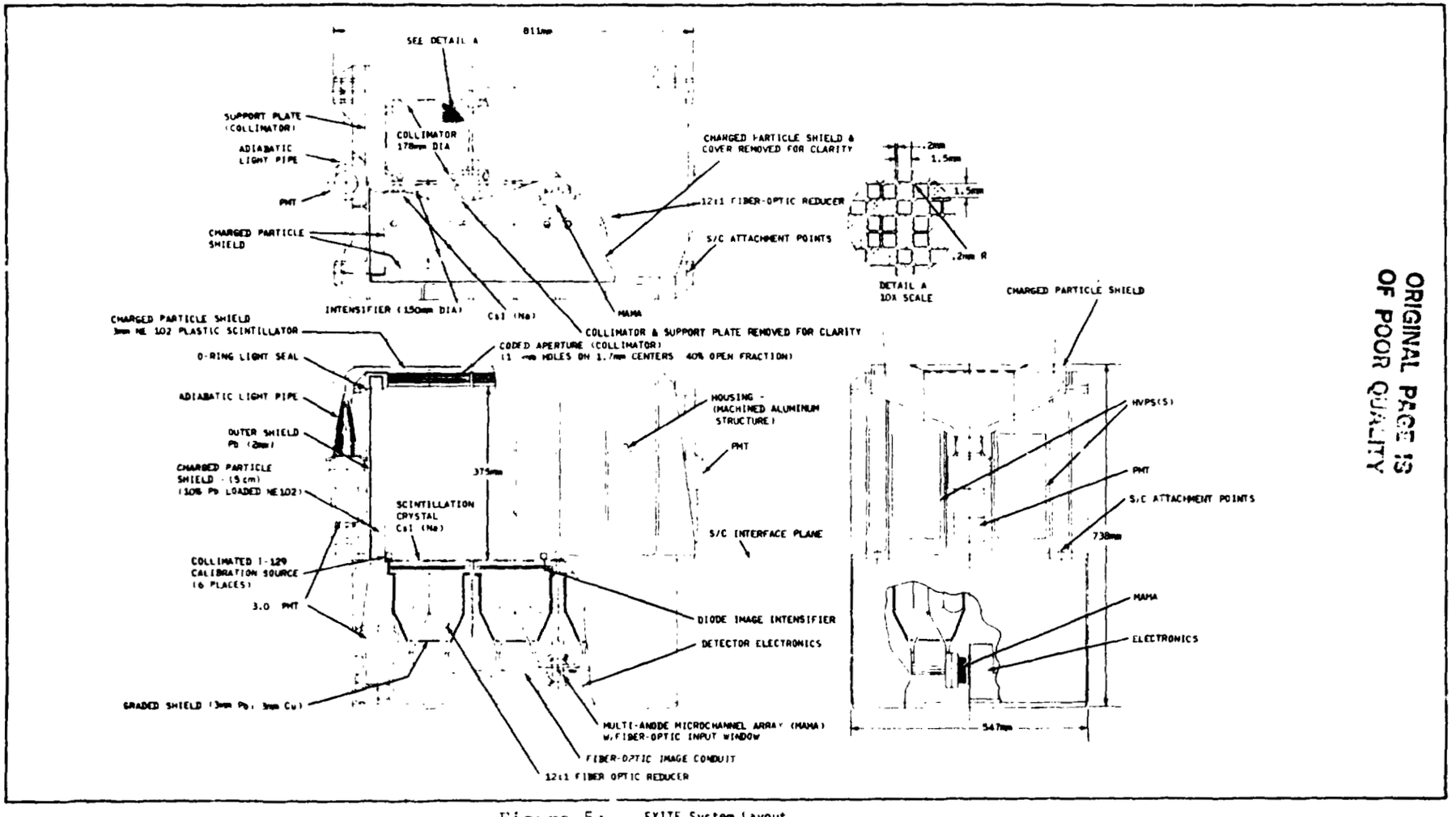

Figure 5: EXITE System Layout

ORIGINAL PAGE IS
OF POOR QUALITY

(~15 μm), each electron will be independently amplified in the microchannel plate (MCP) array (with gain ~10^7) and the total charge coming out of the plate will be proportional to the incident number of photoelectrons and thus the primary X-ray energy. This will be measured using a separate amplifier at the output of the MCP to provide energy information (64 channel PHA). Single electron events due to thermal generation either in the MAMA or the image intensifier can easily be discriminated against using the total charge output from the MCP since a 20 KeV X-ray is expected to produce at least 20 photoelectrons.

EXITE is a modular detector concept. As proposed for XTE, two independent MAMA detectors (each viewing three 15 cm diameter scintillator X-ray detectors) are included for maximum area and the desired redundancy against single point failures. Each detector, however, is actually composed of three independent and parallel scintillators (for maximum usage of the 25 mm circular photocathode area of the MAMAs), and each single 15 cm diameter scintillator operates (in the coded aperture imaging) as a mosaic of adjacent but independent image-forming subdetector elements. All detector subelements (each is 2.2 cm x 1.9 cm) view the same 2.9° (FWHM) field of view on the sky. Thus, each of the two MAMA detector systems is itself actually multiredundant while at the same time easy to test, calibrate, and read out as a single device.

The EXITE design for XTE has a total active detection area of A_{eff} = 438 cm^2 (= geometric area times 0.4 transmission of the collimating coded aperture mask). The detector employs both active and passive shielding to reject and reduce background. The system is shown in Figure 5 above and occupies an area of 81 cm x 54 cm and height (above the spacecraft interface) of 40 cm. It weighs 237.9 kg and requires 3.3 Kbps (max.) of telemetry and 39 watts of power.

Anticipated EXITE Performance

A full simulation of the EXITE detector and optical imaging characteristics has been carried out. Comparison of the EXITE detector system with that (Matteson 1978) flown on HEAO-A4 indicates the total background count rate in the ~15-300 KeV band should be ~35 counts sec^{-1} outside the SAA. Model source spectra were allowed to be incident (on axis) on the full system for a given integration time and were "detected" with the complete system efficiencies and a gaussian blurring (σ = 0.5 pixel) in the centroid determination.

Images of Cyg X-1 for a short (10 sec) and long (500 sec) exposure and of 3C273 for a long (5 x 10^4 sec) exposure are shown in Figure 6 as they should appear from EXITE. These images contain the full 15-300 KeV bandwith of the instrument; similar images could be shown for any band. The full 13 x 11 pixel (2.9°) image is shown; each pixel is 15 arcmin. The sources are detectable in a ~1 pixel radius about the center due to blurring in the MAMA detector readout;

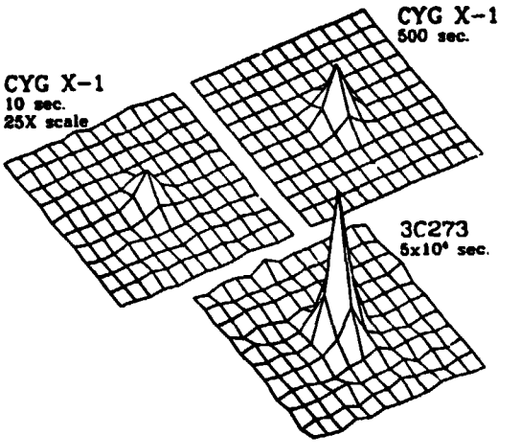

Figure 6: Images (15-300 keV) from Simulated EXITE Data

centroiding is then possible and (for the long exposures) would yield positions with 2 arcmin accuracy. Additional sources in the field which were up to 86 times fainter than Cyg X-1 and ~42 times fainter than 3C273 would be detectable (and located to ~5 arcmin) in the two "long" exposure images, respectively. The total detected count rate of Cyg X-1 by EXITE is 110 counts sec^{-1} while 3C273 is 2.8 counts sec^{-1}. Since Cyg X-1 is the brightest known (steady) source in the ~20-300 KeV energy band, the 100 counts sec^{-1} allowed for in the telemetry has been selected.

The spectra of counts detected in both long exposures are shown in Figure 7 as the plotted points (with actually "observed" 1σ error bars). Also plotted as lines are the assumed input (power law) spectra for both sources. The spectral indices could be derived from the data for either source with uncertainties $\Delta\alpha/\alpha$ of only a few percent.

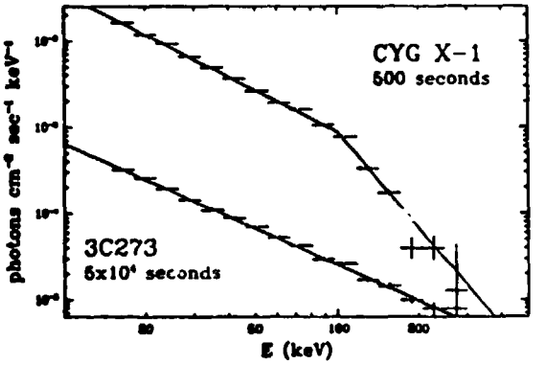

Figure 7: Spectra Derived from Simulated Images.

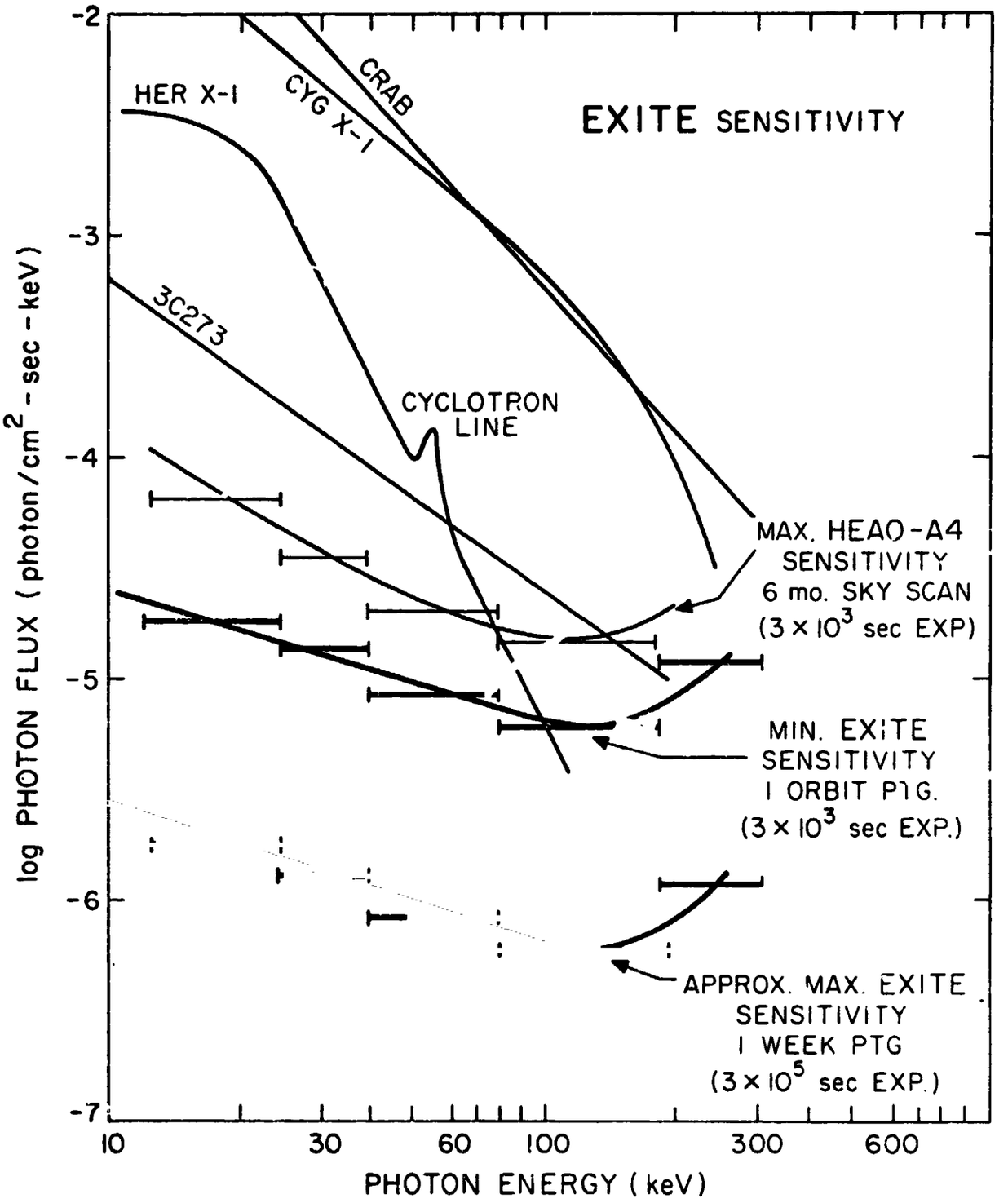

Figure 8: EXITE Sensitivities for 5σ Detection.

The overall sensitivity which EXITE should achieve is shown in Figure 8 for both single orbit (~3000 sec) and ~ 1 week (~3 x 10^5 sec) exposure times. The sensitivity is about a factor of 3-30 times greater than HEAO-A4, also plotted, and is sufficient to meet the science objectives. Approximately 50 new quasars could be detected as serendipitous sources in XTE pointings and located to ≤5 arcmin. Spectra could thus be measured on a large number of AGNs.

5. GAMMA RAY BURST STUDIES WITH EXITE ON XTE

The proposed EXITE detector on XTE would also enable detailed studies of gamma ray bursts to be made. For the first time, both high sensitivity X-ray (~1-30 KeV) as well as hard X-ray (~15-500 KeV) spectra and timing of gamma bursts could be obtained by the large area proportional counter (LAPC) assumed present on XTE and EXITE instruments, respectively. Since recent (Soviet) experimental evidence (Mazets et al. 1979) for cyclotron and positron annihilation lines from bursts as well as the ~8 sec pulsations from the spectacular March 5, 1979, burst (Cline et al. 1980) point toward a neutron star origin, gamma bursts are more than ever appropriate for study from XTE. Nuclear flash models for gamma bursts can account for many of the essential features (Woosley et al. 1981) of bursts and- because of the requirement for strong magnetic fields--would predict an X-ray (~20 KeV) afterglow for perhaps ~10^3 sec. This afterglow emission may have already been detected by the Vela satellite X-ray detectors (Terrell 1980) but more sensitive X-ray and hard X-ray observations are very much needed. This could be conducted on XTE with the EXITE detector, which would both initially detect gamma bursts and measure their spectrum (~50-500 KeV) and approximate source location (~2°) as well as precisely locate (~2′) and study the afterglow emission. No other gamma burst detector systems now being considered could accomplish such broad band (X-ray through gamma ray) studies (spectra and single-station burst location capability) of gamma bursts.

Burst Detector System

The burst system consists of six identical CsI(Na) scintillation detectors (see Figure 9) mounted externally to the EXITE instrument (or even elsewhere on the spacecraft) in such a way as to provide a constant complete sky survey of X-ray/gamma-ray radiation in the ~50-550 KeV energy range. Each detector assembly is composed of a 15.2 cm square by 0.64 cm thick CsI(Na) scintillator, an adiabatic twisted light pipe, a short 38 mm diameter photomultiplier tube (PMT), and associated electronics. Approximately half of the sky is visible to groups of three adjacent detectors. Burst arrival direction cosines may be computed from the relative rates in these various groups of three detectors. Moderately intense bursts ($\gtrsim 1 \times 10^{-7}$ erg cm^{-2}) can thus be located to within ~2° and a real-time spacecraft slew performed (for events sufficiently close to the XTE pointing direction) to obtain a precise (~2 arcmin) location

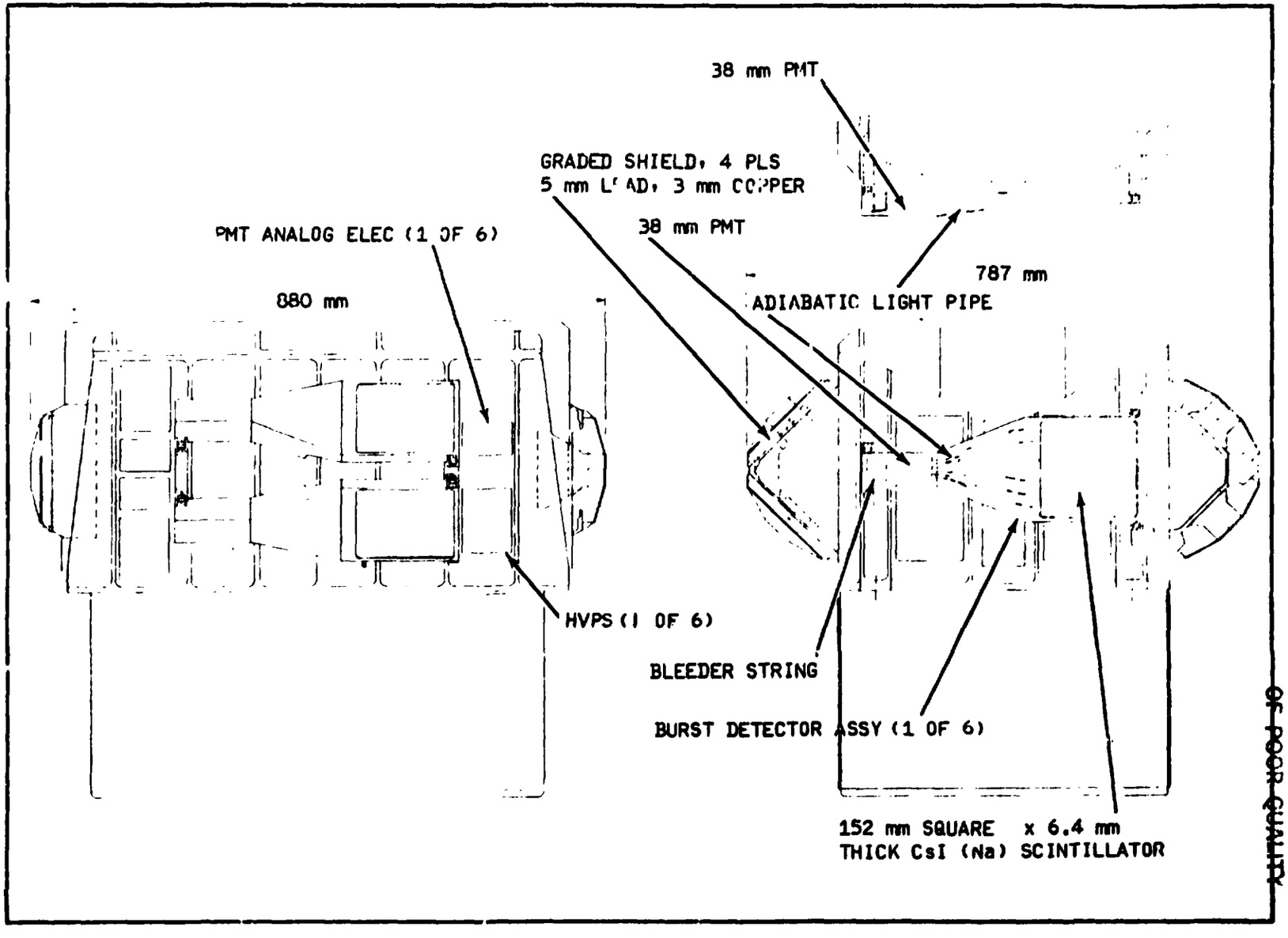

Figure 9: Burst Detector Add On Option.

with the primary EXITE imaging detector system.

For the detectors mounted at 45° to the EXITE shields, a graded shield of lead/copper has been placed on the back side of each scintillator to limit the scintillators to forward viewing only in the gamma-ray energy range below 500 KeV. The window over the front side of all six scintillators is about 1.6 mm thick aluminum. This thickness provides electron shielding to 900 KeV but at the same time only attenuates the X-ray/gamma-ray intensity at 50 KeV by 15 percent (but the high background from lower energy discrete sources and diffuse background is attenuated). Alternatively, a plastic scintillator (~1 cm NE-102) could be mounted on top of the CsI crystals and viewed by the same light pipe and PMT. Particle events could be easily discriminated against by a pulse decay-time discriminator circuit on each detector. Particle-induced burst events are otherwise rejected (in the analysis) by the large area anti-coincidence shields (lead-doped plastic scintillator) on which the burst detector scintillators are mounted (see Figure 8). Rate data from these shields during a burst should also allow the burst radiation scattered from the spacecraft and Earth's atmosphere (thus producing incident particles) to be isolated and the systematic errors in gamma burst arrival directions to be corrected.

Burst Detector Data Handling System

The burst data consists of both high time resolution (0.1 sec) count rates in a fixed band (nominally ~50-300 KeV, but commandable and with a veto for phosphorescence events) and lower time resolution (2 sec) energy spectra (32 channel PHA--~50-550 KeV and 16 bits per channel, or sufficient for even a $\sim 10^{-3}$ erg cm^{-2} burst) for each detector. Each detector event rate contained in the 50 to 300 KeV window is counted into 16 bit counters once every 0.1 seconds. Each counter's content is stored sequentially in memory which has the capability (~0.5 Mbit) to hold three minutes worth of data. The counter data are also routed to a µp subsystem where they are reformatted into 0.3-second samples for the continuous on-going normal telemetry data stream. In addition, the µp continually monitors these six rates via a burst mode algorithm to detect bursts (required in 2 detectors). If a burst is detected, a burst flag is set. The flag has 0.1 second time resolution. A sixteen level command buffer is provided for inflight control of the burst level criterion. As an option, the µp can also use the rate data to calculate the direction cosines of the burst location. These direction cosine values are routed through a special spacecraft interface port for possible use in automatically slewing the spacecraft to point at the burst source.

When a burst is detected, the burst flag is set but the memory continues to accept/spill data for an additional two minutes. At the end of this 2-minute period, the memory contents are frozen and remain frozen until the burst flag is cleared by command. Thus, three minutes of time/energy spectrum burst data, one minute before the flag and two minutes after the flag, are preserved. At the end of the

2-minute period, these memory data are automatically sent to the data stream by usurping the telemetry space normally taken by the prime science (imaging) data and housekeeping data. Approximately 164 seconds are required to transfer all the data to the ground. After the initial dump, additional memory data dumps can be made as desired (by command) until the burst flag is reset.

The total EXITE telemetry is organized in two formats. The normal format contains 0.3 second rate data, coded aperture prime science data, and housekeeping data. In the event of a burst (or if the burst flag is set by command) a burst mode format is set. In this format, the rate data continues as before with 0.3 second samples of the six burst detectors and five CPDs, but the memory dump usurps the 3.298 Kb/sec prime data plus housekeeping data rate long enough to be automatically transmitted at the end of flag plus two minutes, or upon command. When no memory dump is needed, the system reverts back to sending prime imaging data and housekeeping data as in the normal mode.

The weight addition for the Burst Detection System (including added electronics and HVPSs) is estimated at 33.4 kg. The power estimate for the burst detector system electronics is 12 watts.

Burst Detector Sensitivity and Performance

The background detected by the burst system is due to Earth albedo gamma rays and neutrons, spacecraft albedo, activation of the scintillators, diffuse and discrete source background and phosphorescence from charged particle interactions in the scintillators. Above the ~50 KeV threshold, phosphorescence is negligible and the largest background contribution for these wide-angle detectors is from atmospheric and spacecraft albedo. Using results from Ling (1975) and Trombka et al. (1973) for these components, respectively, and allowing for a factor of ~2 uncertainty, we estimate a total background spectrum $dN/dE \simeq 2.6\ E^{-0.9}$ cts/cm^2 sec KeV in the ~50-300 KeV band. This gives a total average background count rate $B \simeq 1700$ cts/sec in each of the six detectors. For orbits transiting the SAA (approximately one-third of the orbits), this average rate will increase substantially (factor of ~2-3) due to long-lived (~0.5 hour) activation decays. An increased effective background rate, incorporating the SAA duty cycle, has been used in deriving the sensitivities below.

Using the typical gamma burst spectra derived by Cline and Desai (1975) the total signal count rate expected in each detector is $S \simeq 3.7 \times 10^4$ cts/sec for a burst with total energy 10^{-4} erg cm^{-2} and assumed ~1 sec (peak) duration. Thus, the threshold for (5σ) burst detection (in three detectors) should be for energies $>4 \times 10^{-7}$ erg cm^{-2}. This is the approximate threshold for coarse ~20° positions and log N - log S studies. To achieve ~2° burst positions (and high S/N spectra to search for line features), a signal-to-noise ratio of >30 is required in each of three detectors.

This should occur for bursts larger than ~1.0 x 10^{-5} erg cm^{-2}, which are expected (from present log N-log S results) at a rate of ~40 per year within the ~2π steradians for which accurate locations can be derived. (Note that although bursts are detectable with approximately all-sky coverage, accurate locations are possible for about half the sky.) Thus, even if XTE slews could only be carried out within a ~1000 sec afterglow period for burst directions within ~45° of the pointing position, ~10 bursts per year would be accurately located by EXITE and observed with high sensitivity by EXITE and the LAPC. We note that estimates by Woosley et al. (1981) for the afterglow spectrum ($L_x \simeq 10^{35}$ erg s^{-1}, $kT \simeq 20$ KeV) would predict EXITE sensitivities of ~25σ per second for a typical burst source at ~500 pc distance. Thus, high signal-to-noise spectra and timing observations should be possible.

Finally, the EXITE burst detection system could detect (5σ) persistent hard X-ray sources with strengths ~1/3 Crab and a Crab-like spectrum in ~300 sec. Thus, hard sources can be monitored continuously and an all-sky monitor capability provided for XTE.

REFERENCES

Calabro, D. and Wolf, J. 1968, Inform Control, 11, 537.

Cline, T. and Desai, U. 1975, Ap. J. (Letters), 196, L43.

Cline, T.L., et al. 1980, Ap. J. (Letters), 237, L1.

Dicke, R. 1968, Ap. J. (Letters), 153, L101.

Fenimore, E. 1980, Applied Optics, 19, 2465.

Gunsen, J. and Polychronopulos, B. 1976, MNRAS, 177, 485.

Kellogg, E., Murray, S.S., and Bardas, D. 1979, IEEE Trans. Nuc. Sci., NS-26, 403.

Ling, J.C. 1975, J Geophys. Res., 80, 3241.

Martin, C., Jelinsky, J., Lampton, M., Malina, R., and Anger, H. 1981, Rev. Sci. Instr., in press

Matteson, J. 1978, AIAA 16th Aerospace Sc. Meeting.

Mazets, E.P., et al. 1979, FTI (Leningrad), Preprint No. 599, 618.

Rocker, G. 1981, these proceedings.

Terrell, J. 1980, Talk at Texas Symposium, Baltimore, MD.

Timothy, J., Mount, G., and Bybee, R. 1979, SPIE-Optics, 183, 169.

Trombka, J., et al. 1973, Ap. J., 181, 737.

Woosley, S., et al. 1981, Preprint.